Analytical Methods

COMMUNICATION

View Article Online
View Journal | View Issue

Cite this: *Anal. Methods*, 2016, **8**, 6682

Received 10th July 2016
Accepted 8th August 2016

DOI: 10.1039/c6ay01963c

www.rsc.org/methods

A fully disposable paper-based electrophoresis microchip with integrated pencil-drawn electrodes for contactless conductivity detection†

Cyro L. S. Chagas,[a] Fabrício R. de Souza,[a] Thiago M. G. Cardoso,[a] Roger C. Moreira,[a] José A. F. da Silva,[b] Dosil P. de Jesus[b] and Wendell K. T. Coltro*[a]

We describe for the first time the fabrication of a paper-based microchip electrophoresis (pME) device with integrated hand-drawn pencil electrodes to perform capacitively coupled contactless conductivity detection (C^4D). This low-cost device (less than $0.10) revealed great capability to dissipate heat, good injection-to-injection repeatability, and ease of attaching pencil-drawn electrodes on the separation channel. The feasibility of the proposed pME-C^4D device was successfully demonstrated with the separation of bovine serum albumin and creatinine within 150 s with baseline resolution. The limits of detection values for albumin and creatinine were 20 and 35 μmol L^{-1}, respectively. These biomolecules present clinical relevance as evidence of kidney failure. The proposed pME-C^4D offers great potential to be explored in the diagnosis of diabetes mellitus and heart disease.

The use of paper platforms in electrophoresis has been reported since the 1940s as a very useful tool for the separation of amino acids, peptides, and proteins. However, this technique exhibits low resolution, longer analysis time, and several problems related to detection and quantification of analytes.[1–4] These facts have made the traditional paper electrophoresis unpopular nowadays and pushed the use of this substrate towards conventional analytical techniques such as filtration and clinical applications such as pregnancy tests.[5] Recently, Whitesides' research group introduced the concept of microfluidic paper-based analytical devices (μPADs) as a bioanalytical platform to measure glucose and protein concentration levels.[6] μPADs bring the idea of minimum reagent waste as well as operational simplicity, revealing the necessity of improving the portability and reducing the cost of analysis.[6–9]

The advent of μPADs has contributed to the return of paper as a platform for electrophoresis separations with the aim of rapid and low-cost analysis. In 2014, Ge *et al.* reported the electrophoretic separation of serine, aspartic acid, and lysine on a paper-based device using an on-column wireless electrogenerated chemiluminescence detector.[10] In the same year, Luo *et al.* developed a low-voltage, origami paper-based electrophoresis device to analyze fluorescent molecules and serum proteins with fluorescence detection.[11] Despite the innovation of these two pioneering reports, some parameters such as sample injection control, separation quality, and robustness still need to be improved in paper electrophoresis. To this end, Xu and co-workers developed a paper-based electrophoresis device containing injection and separation channels arranged in a cross-shaped format, allowing the electrokinetic injection of the sample based on the floating mode.[12] The separation of two organic dyes was monitored using a digital camera or cell phone camera and completed within 10 min.

Along with the remarkable applications of this low-cost microfluidic platform, the development of electrochemical paper-based devices has received considerable attention in the last five years. Since the first reports,[13–15] paper has become increasingly popular as a substrate in the production of conductive paths by using microwires, sputtering, screen printing or simply hand-drawing methods.[14,16–20] Examples showing the integration of amperometric detection on μPADs to monitor chromatographic separations have been successfully explored.[16,17] Among the electrochemical detection methods, capacitively coupled contactless conductivity detection (C^4D) has emerged as a powerful system to be integrated on chip-based electrophoresis devices.[18–23] The growing attention devoted to the use of C^4D on electrophoresis microchips has been promoted by its advantages over "contact mode", including the electrical insulation between sensing electrodes and fluidic channels, which eliminates electrical interferences from the high electric field used during electrophoretic runs.

In this context, the main goal of this communication aims to describe for the first time the development of a fully disposable

[a]*Instituto de Química, Universidade Federal de Goiás, 74690-900, Goiânia, Goiás, Brazil. E-mail: wendell@ufg.br*

[b]*Instituto de Química, Universidade Estadual de Campinas, 13083-970, Campinas, São Paulo, Brazil*

† Electronic supplementary information (ESI) available. See DOI: 10.1039/c6ay01963c

paper-based microchip electrophoresis (pME) device with integrated pencil-drawn electrodes for C^4D. This pME-C^4D device was evaluated as an alternative for the separation of albumin and creatinine, which are the main biomarkers in the detection of kidney disease.

Modern instrumental analytical chemistry has actively contributed towards the development of clinical diagnostics, aiming at the need for affordable and low-cost clinical tests. According to the World Health Organization, in 2012, diabetes and cardiovascular diseases are among the four major causes of death in the world.[24] Proteinuria is defined as an excessive protein loss in the urine or an abnormal protein concentration in the serum. This symptom indicates a kidney lesion generally caused by other dysfunctions in human body, such as diabetes mellitus, cardiovascular disease, or high blood pressure.[25] The most common methods for detecting proteinuria are based on colorimetry and immunochemistry assays. The colorimetric approach is based on strip tests, which is a semi-quantitative method due to its low accuracy. In addition, it is operator-dependent and may provide a false positive result depending on the sample conditions. On the other hand, the immunochemistry tests present high sensitivity, specificity, and reproducibility. The main limitations involve the cost and the required instrumentation and facilities.[25–29]

The fabrication process of pME devices is represented in Fig. 1. Firstly, the pME layout, arranged in a simple cross-shape geometry (Fig. 1a), was drawn in a graphical software (CorelDraw Graphics Suite v. X6). Injection and separation channels (1 mm wide and 100 μm high) were 26 and 60 mm long, respectively. The desired layout was then cut in a Whatman chromatographic paper (Grade 01) using a CO_2 laser engraver at a local printing service (Ordones Laser Ltd., Goiânia, GO, Brazil). After the cutting step, the pME device was thermally laminated with thermal laminating pouches (Fig. 1b). As can be seen in Fig. 1c, the bases of micropipette tips were used to create reservoirs for buffer (B), sample (S), sample waste (SW), and buffer waste (BW). Solution reservoirs were glued on the device top using a bicomponent epoxy resin. Electrodes for C^4D measurements were drawn on paper with graphite pencil as described by Chagas and co-workers[30] and attached to the pME using an adhesive tape. The detection cell, composed of two electrodes for excitation (e0) and reception (e1), was designed in an antiparallel orientation (2.0 mm wide, 2.0 cm long) with gap of 1 mm and attached on the pME device as depicted in Fig. 1c.

Electrophoresis experiments on the pME-C^4D devices were carried out using a bipolar two-channel high-voltage sequencer. Microfluidic channels were filled by capillary action with running buffer in B, S, and SW reservoirs, while the BW reservoir was left empty. Afterwards, the BW reservoir was filled with running buffer, the high voltage platinum electrodes were immersed into each reservoir, and the channels were electrokinetically conditioned with running buffer for 10 min each to ensure their complete filling, without the presence of air bubbles. To proceed with sample electrokinetic injection based on floating mode, all solutions in reservoirs were renewed, and the sample was added in the sample reservoir. After application of the desired voltage in the injection channel for 50 s, the voltage was switched to the separation channel. In this way, the sample zone defined at the channel intersection was introduced into the separation channel.

Prior to proceeding with the study on electrophoretic performance, the electrical resistance of the microchannel produced on paper was determined based on current *versus* voltage plot. Paper channels were firstly filled with a running

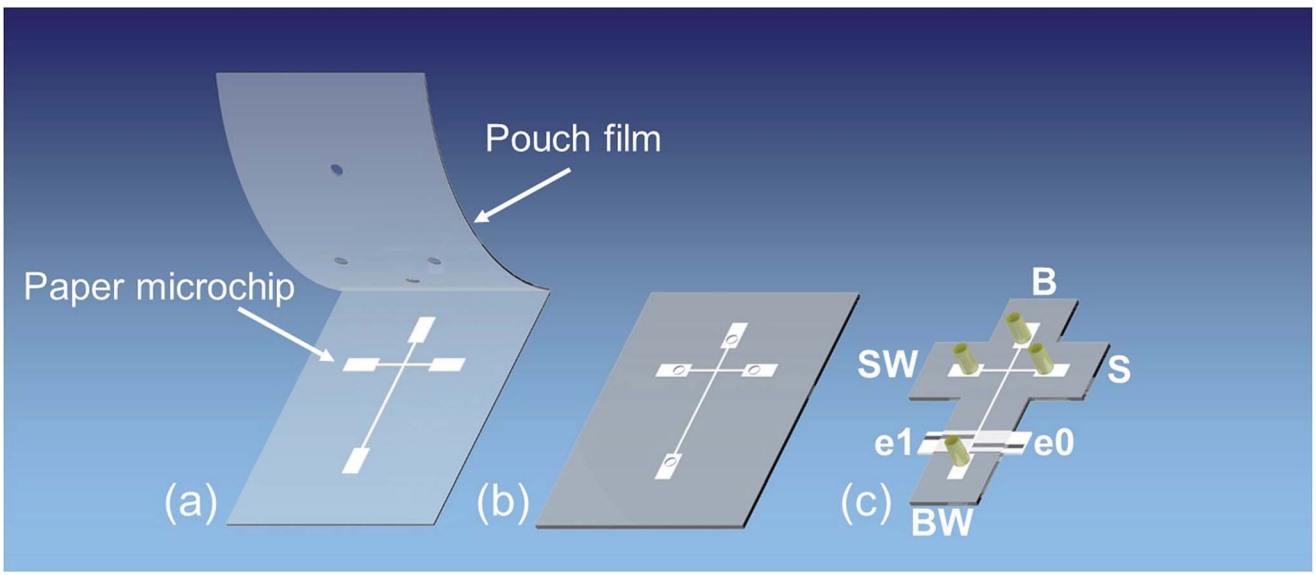

Fig. 1 Fabrication process of paper-based microchip electrophoresis (pME) with integrated electrodes for C^4D measurements. Images (a–c) show the positioning of paper microchip between the two layers of pouch film, the laminated device, and the resulting fully integrated pME-C^4D device containing pencil-drawn electrodes and solution reservoirs. In (c), the labels S, SW, B, BW, e0 and e1 mean reservoirs for sample, sample waste, buffer, buffer waste, and excitation and receiver electrodes, respectively.

buffer composed of 2-(*N*-morpholino)ethanesulfonic acid (MES) and histidine (His) (20 mmol L^{-1} each, pH 6.1). Then, voltage was applied to the injection channel ranging in magnitude from +0.6 kV to +3.0 kV (0.2 kV increments). The current *versus* voltage plot exhibited a linear behavior with correlation coefficient equal to 0.994 (see ESI, Fig. S1†). The electrical resistance, calculated based on the reciprocal of Ohm's plot slope, was estimated to be 130 ± 18 MΩ. This value is greater than the electrical resistance achieved for PDMS chips under the same conditions (data not shown). Based on the found data, it is possible to conclude that the paper microchannels evidenced an ohmic behavior and provided effective heat dissipation.

Once their excellent capability to dissipate heat was demonstrated, the coupling of electrodes on pME was studied. For this purpose, electrodes for C^4D measurements were coupled to pME in three different arrangements, including top, bottom, and top–bottom positions (see Fig. 2a), to find the best signal-to-noise ratio (SNR) and peak symmetry. The comparison of the analytical response with these three detection cells was performed with the electrokinetic injection of a solution containing 500 μmol L^{-1} Na^+. A 300 kHz sinusoidal wave with 1.0 $V_{peak\text{-}to\text{-}peak}$ amplitude was applied to the excitation electrode, and the resulting current was then converted to voltage and monitored in a LabVIEW® software. A sequence of five electropherograms was recorded for each electrode configuration (see ESI, Fig. S2†), and according to the results achieved for peak area, intensity, and separation efficiency (see ESI, Table S1†), the best configuration for coupling the electrodes is the bottom side of the separation channel. In this configuration, the electrodes are better isolated in comparison with other configurations because they are positioned between the pME device and a PDMS base, thus suffering lower external interference, corroborating for the best data. The slight shift on the migration times may be associated with small variations during the positioning of electrodes for the different geometries.

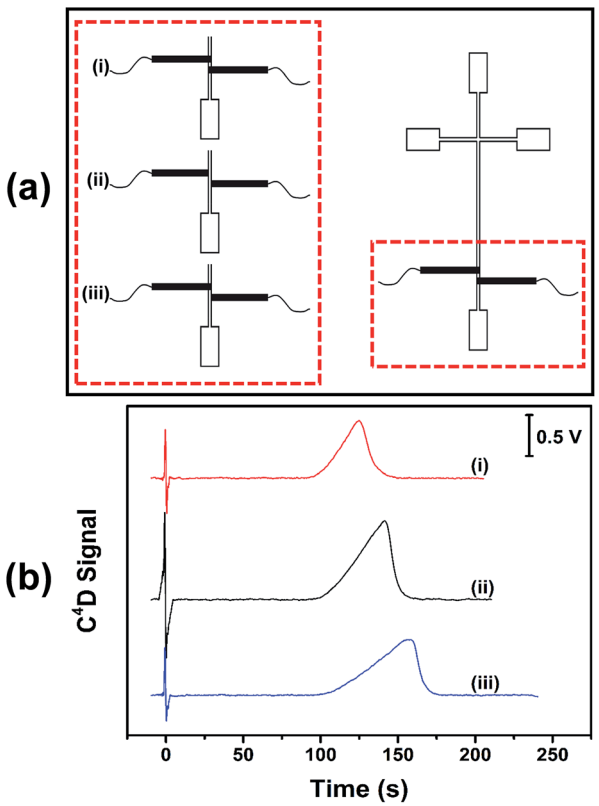

Fig. 2 Presentation of (a) modes for attaching electrodes on paper separation channel and (b) resulting electropherograms for the injection of Na^+ (500 μmol L^{-1}). Three different electrode attaching modes were evaluated for the conductivity detection cell: (i) both electrodes on the top foil layer, (ii) both electrodes on the bottom foil layer, and (iii) electrodes were placed on different foil layers – one on the top and the other on the bottom. Floating injection: 2.3 kV/50 s. Separation voltage: 2.5 kV. Detection: 300 kHz sinusoidal wave with 1.0 V_{pp} amplitude. Other experimental conditions: see text.

While the position of electrodes at the bottom side of pME has provided the highest peak intensity, the use of top–bottom arrangement exhibited the broadest peak. According to the results depicted in Fig. 2b, the detection cell was attached on bottom side of pME devices and kept for subsequent assays. The electrokinetic injection through floating mode on pME devices provided satisfactory precision for a series of ten consecutive injections (see ESI, Fig. S3†). The achieved results provided RSD values for Na^+ (250 μmol L^{-1}) peak intensity and area of 7.2% and 9.2%, respectively. The good injection-to-injection repeatability achieved on pME devices during a longer injection time (50 s) in comparison with other electrophoretic microsystems proves that the floating injection mode is suitable for use in the proposed analytical devices.

After establishing the best detection electrode arrangement and ensuring good precision of electrokinetic injection on pME chips, the feasibility of the proposed devices was studied in the electrophoretic separation of bovine serum albumin (BSA) and creatinine. These analytes were selected due to their clinical relevance in the diagnosis of diabetes mellitus and heart diseases. Normally, human serum albumin (HSA) instead of BSA is more suitable for this kind of diagnosis. However, both proteins exhibit similar physical characteristics and electrophoretic behaviors.[31,32] For this reason, the choice of BSA to demonstrate the proof-of-concept for the proposed microfluidic device is acceptable. Firstly, the running electrolyte was optimized, and the best separations were obtained using a mixture of 20 mmol L^{-1} lactic acid and 2 mmol L^{-1} His (pH 3.1). Fig. 3 shows the series of three injections for a mixture of both biomolecules prepared in a concentration range between 100 and 300 μmol L^{-1} each.

As can be seen, the electropherograms exhibited well-defined peaks with baseline resolution for all concentrations. The attained resolution ranged between 1.6 and 1.8. The separation efficiencies calculated for BSA and creatinine were 2900 ± 160 and 4700 ± 380 plates per meter, respectively. These efficiency values are relatively low when compared to those generally obtained with conventional microchip electrophoresis. This reduced separation efficiency can be related to the channel dimensions as well as the porous media associated with the paper platform for electrophoresis. The migration times proved to be very reproducible, with RSD lower than 2% for both analytes.

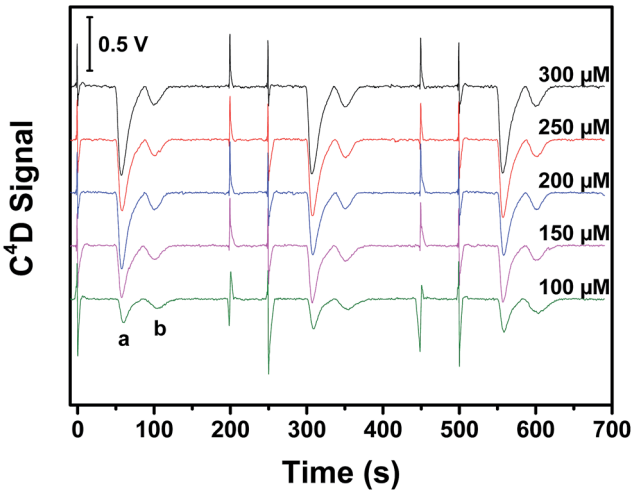

Fig. 3 Sequential electropherograms showing the separation of (a) bovine serum albumin and (b) creatinine at five concentration levels. Experimental conditions: see Fig. 2.

Regarding the experimental conditions selected in this current study, it is important to highlight that creatinine presented lower electrophoretic mobility than albumin. The migration order can be explained through the observation of albumin and creatinine hydrophilicity. Some studies using chromatography reported that in separations of urinary compounds, creatinine normally is the first analyte to elute on a reversed-phase column (nonpolar).[33,34] The hydrophilic characteristic of paper corroborates with the late migration of creatinine instead of albumin once creatinine exhibits higher hydrophilicity in comparison with albumin. The calibration curves for both analytes presented linear behavior in terms of peak areas (see ESI, Fig. S4†). However, the achieved determination coefficient for creatinine was lower than that observed for BSA. In addition, a small variation was observed on the output voltage during C^4D measurements for the creatinine concentration range between 100 and 300 μM. The lower response in terms of peak intensity and area for creatinine may be attributed to the partial ionization at the pH of the running buffer. In addition, the noticeable standard deviation values for successive injections ($n = 3$) as well as the observed deviation of linearity may also be related to the biased electrokinetic injection, which discriminates the injected amount of analytes according to their electrophoretic mobilities as well as the electroosmotic flow (EOF) magnitude.[35] Taking into account the SNR equal to 3, the LOD calculated for BSA and creatinine were 20 and 35 μmol L^{-1}, respectively. These values are typically below the concentration levels achieved in real samples. Therefore, the proposed device has great potential to be used in the separation of these biomolecules, allowing the correlation of their concentration with clinical studies related to kidney diseases. Analysis of human artificial serum with normal levels of BSA and creatinine was performed, and the recorded electropherograms are presented in ESI, Fig. S5.† Due to the high conductivity of artificial serum sample, lower separation potential was used (2.3 kV), allowing the complete separation of BSA and creatinine within 250 s. In addition, the albumin peaks are partially overlapped with another peak not observed in standard mixture. This can be attributed to the complexity of the serum sample. The composition of artificial serum sample is presented in Table S2, available in the ESI.†

In order to support the proposed pME devices, we performed the same separation on commercial glass electrophoresis microchips coupled with C^4D under similar electrophoretic conditions. Despite the identical running conditions, experiments on pME and glass devices were performed in different systems. While separations on pME were carried out in a homemade system, the use of glass chips was evaluated in a commercial equipment.[36] For this reason, the output voltages recorded in both C^4D systems are on different scales. The electropherograms containing injections of (i) creatinine, (ii) BSA, and (iii) creatinine + BSA are available in the ESI, Fig. S6.† It is important to note that when a mixture of two analytes was injected, only one peak was observed. Based on these results, it can be inferred that in free solution microchip electrophoresis, complex formation between BSA and creatinine occurs due to the capacity of BSA to bind with some molecules, including those having amine groups.[33,34]

In addition to the capability to promote the separation of creatinine and albumin on pME devices, the presence and magnitude of the EOF was investigated based on the current monitoring method.[37] The value found on the paper substrate explored for the separations previously demonstrated, designated as native paper, was equal to $1.7 \pm 0.3 \times 10^{-6}$ cm^2 V^{-1} s^{-1}. Different types of paper, including oxidized and silica-coated surfaces, have been recently used for bioanalytical studies;[38,39] the EOF magnitude was estimated on pME devices fabricated on these substrates and compared to the native surface. For this purpose, we used the chromatographic paper previously oxidized sodium periodate[38] and commercial silica-coated ion-exchange paper (grade SG81).[39] The EOF values obtained for oxidized and silica-coated papers were $1.2 \pm 0.4 \times 10^{-4}$ cm^2 V^{-1} s^{-1} and $2.2 \pm 0.2 \times 10^{-4}$ cm^2 V^{-1} s^{-1}, respectively. The enhanced EOF values can be attributed to the largest density of negative charge at the paper surface when compared to the native substrate. The EOF achieved for the native paper device at pH 3.1 is *ca.* two orders of magnitude lower than other substrate materials usually selected for chip-based electrophoresis applications, while the EOF for oxidized and silica-coated paper devices were similar to the glass ME devices,[40] for example.

In summary, we described for the first time the development of disposable paper-based electrophoresis microchips integrated with pencil-drawn electrodes to conduct C^4D measurements and monitor electrophoretic separations of bovine serum albumin and creatinine. All the fabrication steps were demonstrated to be quite simple, including the cutting of paper channels, the drawing of sensing electrodes, as well as integration based on thermal lamination. Moreover, the production of integrated pME-C^4D does not require cleanroom facilities and demands only globally affordable consumables like paper sheets, graphite pencil and laminating pouches. The achievements reported in this study bring back the paper platform for

electrophoretic separations of biomolecules, in which the paper substrate can be selected based on its properties as well as according to the EOF magnitude. The proposed pME-C^4D device offers several attractive features such as low cost, portability, disposability and, most importantly, great capacity to promote electrophoretic separations of clinically relevant compounds, opening new prospects for clinical analysis on paper, as in the detection of kidney dysfunctions, for example.

Acknowledgements

The authors gratefully thank financial support from CNPq (grants 448089/2014-9, 444514/2014-7 and 311744/2013-3), CAPES (grants 3363/2014 and 802-14), FAPEG, FAPESP (grant 2013/22127) and INCTBio. This study is dedicated to the memory of Dr Craig Lunte.

References

1 H. G. Kunkel and A. Tiselius, *J. Gen. Physiol.*, 1951, **35**, 89–118.
2 W. P. Jencks, M. R. Jetton and E. L. Durrum, *Biochem. J.*, 1955, **60**, 205–215.
3 W. Mejbaum-Katzenellenbogen and W. M. Dobryszycka, *Clin. Chim. Acta*, 1959, **4**, 515–522.
4 P. G. Righetti, *J. Chromatogr. A*, 2005, **1079**, 24–40.
5 J. R. Ehrenkranz, *Epidemiology*, 2002, **13**, S15–S18.
6 A. W. Martinez, S. T. Phillips, M. J. Butte and G. M. Whitesides, *Angew. Chem., Int. Ed.*, 2007, **46**, 1318–1320.
7 W. K. Tomazelli Coltro, C. M. Cheng, E. Carrilho and D. P. Jesus, *Electrophoresis*, 2014, **35**, 2309–2324.
8 D. M. Cate, J. A. Adkins, J. Mettakoonpitak and C. S. Henry, *Anal. Chem.*, 2015, **87**, 19–41.
9 M. Santhiago, E. W. Nery, G. P. Santos and L. T. Kubota, *Bioanalysis*, 2014, **6**, 89–106.
10 L. Ge, S. Wang, S. Ge, J. Yu, M. Yan, N. Li and J. Huang, *Chem. Commun.*, 2014, **50**, 5699–5702.
11 L. Luo, X. Li and R. M. Crooks, *Anal. Chem.*, 2014, **86**, 12390–12397.
12 C. Xu, M. Zhong, L. Cai, Q. Zheng and X. Zhang, *Electrophoresis*, 2016, **37**, 476–481.
13 W. Dungchai, O. Chailapakul and C. S. Henry, *Anal. Chem.*, 2009, **81**, 5821–5826.
14 R. F. Carvalhal, M. Simão Kfouri, M. H. de Oliveira Piazetta, A. L. Gobbi and L. T. Kubota, *Anal. Chem.*, 2010, **82**, 1162–1165.
15 Z. Nie, C. A. Nijhuis, J. Gong, X. Chen, A. Kumachev, A. W. Martinez, M. Narovlyansky and G. M. Whitesides, *Lab Chip*, 2010, **10**, 477–483.
16 L. Y. Shiroma, M. Santhiago, A. L. Gobbi and L. T. Kubota, *Anal. Chim. Acta*, 2012, **725**, 44–50.
17 N. Dossi, R. Toniolo, E. Piccin, S. Susmel, A. Pizzariello and G. Bontempelli, *Electroanalysis*, 2013, **25**, 2515–2522.
18 M. Pumera, *Talanta*, 2007, **74**, 358–364.
19 W. K. T. Coltro, R. S. Lima, T. P. Segato, E. Carrilho, D. P. de Jesus, C. L. do Lago and J. A. F. da Silva, *Anal. Methods*, 2012, **4**, 25–33.
20 P. Kubáň and P. C. Hauser, *Electrophoresis*, 2015, **36**, 195–211.
21 J. A. Fracassi da Silva and C. L. do Lago, *Anal. Chem.*, 1998, **70**, 4339–4343.
22 M. Pumera, J. Wang, F. Opekar, I. Jelínek, J. Feldman, H. Löwe and S. Hardt, *Anal. Chem.*, 2002, **74**, 1968–1971.
23 J. Wang, M. Pumera, G. Collins and I. Jelínek, *Analyst*, 2002, **127**, 719–723.
24 World Health Organization, http://www.who.int/mediacentre/factsheets/fs310/en/index2.html, accessed on April 25, 2016.
25 C. Burtis, *Tietz Fundamentos da Química Clínica*, Elsevier Brasil, 2011.
26 D. Newman, H. Thakkar and H. Gallagher, *Clin. Chim. Acta*, 2000, **297**, 43–54.
27 M. T. Wu, K. K. Lam, W. C. Lee, K. T. Hsu, C. H. Wu, B. C. Cheng, H. Y. Ng, P. J. Chi, Y. T. Lee and C. T. Lee, *J. Clin. Lab. Anal.*, 2012, **26**, 82–92.
28 V. Lezaic, in *Biomarkers in Kidney Disease*, ed. B. V. Patel, Springer Netherlands, Dordrecht, 2015, pp. 1–18, DOI: 10.1007/978-94-007-7743-9_31-1.
29 A. E. Merrill, J. Khan, J. A. Dickerson, D. T. Holmes, N. S. Harris and D. N. Greene, *Clin. Chim. Acta*, 2016, **460**, 114–119.
30 C. L. S. Chagas, L. Costa Duarte, E. O. Lobo-Júnior, E. Piccin, N. Dossi and W. K. T. Coltro, *Electrophoresis*, 2015, **36**, 1837–1844.
31 I. Miller and M. Gemeiner, *Electrophoresis*, 1993, **14**, 1312–1317.
32 A. Michnik, K. Michalik, A. Kluczewska and Z. Drzazga, *J. Therm. Anal. Calorim.*, 2005, **84**, 113–117.
33 J. Zhao, H. Chen, P. Ni, B. Xu, X. Luo, Y. Zhan, P. Gao and D. Zhu, *J. Chromatogr. B: Anal. Technol. Biomed. Life Sci.*, 2011, **879**, 2720–2725.
34 C. Burton, H. Shi and Y. Ma, *Anal. Chem.*, 2013, **85**, 11137–11145.
35 M. Blas, N. Delaunay and J. L. Rocca, *Electrophoresis*, 2008, **29**, 20–32.
36 C. B. Freitas, R. C. Moreira, M. G. de Oliveira Tavares and W. K. Coltro, *Talanta*, 2016, **147**, 335–341.
37 X. Huang, M. J. Gordon and R. N. Zare, *Anal. Chem.*, 1988, **60**, 1837–1838.
38 P. de Tarso Garcia, T. M. G. Cardoso, C. D. Garcia, E. Carrilho and W. K. T. Coltro, *RSC Adv.*, 2014, **4**, 37637–37644.
39 Q. Wang, Y. Zheng, X. Zhang, X. Han, T. Wang and Z. Zhang, *Analyst*, 2015, **140**, 8048–8056.
40 W. K. T. Coltro, S. M. Lunte and E. Carrilho, *Electrophoresis*, 2008, **29**, 4928–4937.

